

**SYNTHESIS AND CHARACTERIZATION OF LANTHANIDE-BENZOATO  
COMPLEXES**

**BY**

**OOI PING HOWE**

**Thesis submitted in fulfilment of the  
Requirements for the degree of  
Master of Science**

**OCTOBER 2011**

*Dedicated to my family*

## ACKNOWLEDGEMENTS

I wish to thank my advisor, Professor Teoh Siang Guan for his intellectual support and continual encouragement throughout my studies. The thesis is made possible by his patience and persistence.

I thank Professor Fun Hoong-Kun, Mr. Goh Jia Hao and Mr. Yeap Chin Sing from School of Physics, USM for their help and guidance in solving crystal structure for the complexes.

I am grateful to Mr. Aw Yeong Cheok Hoe, Mr. Marimuthu, Mr. Ong Chin Hin, Mr. Razly Effendy, Miss Ami Mardiana Bt. Othman, Mr. Mohamed Mustaqim Abu Bakar, Miss Siti Khadijah Mohd. Bakhori for their guidance in sample analyzing and characterization.

I also wish to thank Assoc. Professor Dr. Tan Soo Choon, Ms. Wan Raihana Wan Aasim, Ms. Tan Yifen, Ms. Tan Yuen Lin, Mr. Sim Hann Liang, Ms. Karen Ong and other friends for moral support, without which this thesis would not be possible.

## TABLE OF CONTENTS

TABLE OF CONTENTS.....	iv
LIST OF TABLES.....	ix
LIST OF FIGURES .....	xii
LIST OF ABBREVIATIONS/SYMBOL .....	xv
LIST OF APPENDICES.....	xvi
ABSTRAK.....	xvii
ABSTRACT.....	xviii
CHAPTER 1 INTRODUCTION.....	1
1.1 History.....	1
1.2 General Information about Lanthanides.....	3
1.2.1 Oxidation States .....	3
1.2.2 Ionic Radius .....	4
1.2.3 Magnetic Properties.....	5
1.2.4 Optical Properties.....	6
1.2.5 Toxicity.....	7
1.2.6 Occurrence .....	8
1.3 Lanthanide Luminescence .....	9
1.3.1 Sensitized Luminescence.....	11
1.3.2 Luminescence Spectroscopy.....	12
1.4 Coordinating Ligands of Lanthanide Complexes .....	14
1.4.1 Carboxylic Acid – General Properties.....	14

1.5	Crystalline Materials and Single Crystals .....	15
1.5.1	Definition of Crystal and Single Crystal .....	15
1.5.2	Crystal Growth Theories.....	16
1.5.3	Solution Growth of Single Crystal.....	17
1.5.4	Hydrothermal Growth/Synthesis.....	17
1.6	Complexation between Carboxylic Acid and Lanthanide .....	18
1.6.1	Coordination Chemistry of Lanthanide .....	18
1.6.2	Hard Soft Acid Base (HSAB) Principle Character of Tripositive Lanthanide Cations ( $\text{Ln}^{3+}$ ) .....	20
1.7	Complexation with Aromatic Carboxylic Acid/1,10-phenanthroline with Lanthanide .....	21
1.8	Research Objective.....	22
	CHAPTER 2 EXPERIMENTAL .....	24
2.1	Materials.. .....	24
2.2	Synthesis Methods.....	26
2.2.1	Synthesis of Lanthanide Carboxylate Complexes.....	26
2.2.1.1	General Synthesis of lanthanides ( $\text{Ln} = \text{Nd}, \text{Sm}, \text{Eu}, \text{Tb}$ ) with benzoic acid and its Derivatives.....	26
2.2.2	Synthesis of Lanthanide Complexes from Benzoic Acid and 1,10- Phenanthroline .....	27
2.2.2.1	Synthesis between neodymium oxide with benzoic acid and 1,10-phenanthroline .....	27

2.2.2.2	Synthesis between europium oxide and terbium oxide with benzoic acid and 1,10-phenanthroline .....	28
2.3	Photosensitivity and Air Stability Evaluation.....	28
2.4	Characterization .....	28
2.4.1	Fourier Transform Infrared Spectroscopy (FTIR) .....	28
2.4.2	CHN Elemental Microanalysis (CHN).....	29
2.4.3	Thermogravimetric Analysis (TGA) .....	29
2.4.4	Photoluminescence Spectroscopy (PL) .....	30
2.4.5	Single Crystal X-ray Diffraction.....	30
CHAPTER 3 RESULTS AND DISCUSSION .....		32
3.1	Physical Appearance, Yield and Ambient Condition Stabilities .....	32
3.2	CHN Elemental Microanalysis .....	35
3.3	Crystal Structures of Lanthanide Complexes with Benzoic Acid and 1,10-Phenanthroline Monohydrate.....	38
3.3.1	Crystal Structure of Tetra- $\mu$ -benzoato- $\kappa^4O:O';\kappa^3O:O,O';\kappa^3O,O':O'$ -bis[(benzoato- $\kappa^2O,O'$ )(1,10- phenanthroline- $\kappa^2N,N'$ )neodymium(III)].....	39
3.3.2	Crystal Structure of Tetra- $\mu$ -benzoato- $\kappa^4O:O';\kappa^3O:O,O';\kappa^3O,O':O'$ -bis[(benzoato- $\kappa^2O,O'$ )(1,10- phenanthroline- $\kappa^2N,N'$ )europium(III)] benzoic acid disolvate .....	45
3.3.3	Crystal Structure of Tetra- $\mu$ -benzoato- $\kappa^4O:O';\kappa^3O:O,O';\kappa^3O,O':O'$ -bis[(benzoato- $\kappa^2O,O'$ )(1,10- phenanthroline- $\kappa^2N,N'$ )terbium(III)] benzoic acid disolvate .....	51

3.4	Fourier Transform Infrared (FTIR) Spectroscopy Studies .....	57
3.4.1	Complexation of Benzoic acid (BA) with Lanthanide salts (Ln = Nd, Eu, Sm and Tb).....	57
3.4.2	Complexation of 2,4-dichlorobenzoic acid (24DCBA) with Lanthanide salts (Ln = Nd, Eu, Sm and Tb) .....	59
3.4.3	Complexation of 3,4-dichlorobenzoic acid (34DCBA) with Lanthanide salts (Ln = Eu, Sm, Nd and Tb) .....	60
3.4.4	Complexation of 4-hydroxybenzoic acid (HBA) with Lanthanide salts (Ln = Nd, Eu, Sm and Tb) .....	61
3.4.5	Complexation of Lanthanide salts (Ln = Nd, Eu and Tb) with BA and 1,10-phenanthroline (PHEN).....	63
3.5	Thermogravimetric Analysis (TGA) .....	65
3.5.1	Thermal stability of free ligands .....	65
3.5.2	Thermal Behavior and Stability of Lanthanide Complexes .....	66
3.5.3	Thermal Behavior and Stability of Ln-BA (where Ln = Eu, Tb, Nd, Sm).....	67
3.5.4	Thermal Behavior and Stability of Ln-24DCBA (where Ln = Eu, Tb, Nd, Sm).....	68
3.5.5	Thermal Behavior and Stability of Ln-34DCBA (where Ln = Eu, Tb, Nd, Sm).....	70
3.5.6	Thermal Behavior and Stability of Ln-HBA (where Ln = Eu, Tb, Nd, Sm).....	71

3.5.7	Thermal Behavior and Stability of Ln-BAPHEN (where Ln = Eu, Tb, Nd).....	72
3.6	PL Emission of Carboxylic Acid and Lanthanide Carboxylates .....	74
3.6.1	PL Emission of the Free Ligand and the Samarium Complexes .....	74
3.6.2	PL Emission of the Eu Complexes.....	78
3.6.2	PL Emission of Europium Complexes .....	79
3.6.3	PL Emission of Terbium Complexes .....	83
3.6.4	PL Emission of Neodymium Complexes .....	88
3.6.5	Summary of PL Emission of the complexes.....	91
CHAPTER 4 CONCLUSION AND RECOMMENDATION FOR FUTURE WORK		93
4.1	Conclusion .....	93
4.2	Recommendation for future work .....	94
BIBLIOGRAPHY.....		96
APPENDIX.....		104
Appendix A: FTIR Spectra Of The Ligand And Their Respective Lanthanide-Benzoato Complexes.....		104
Appendix B: TGA Spectra Of The Ligand And Respective Lanthanide-Benzoato Complexes .....		110

## LIST OF TABLES

Table 1.1: History of the lanthanides (Aspinall, 2001).....	2
Table 1.2: Summary of the properties of Ln(III) ions. ....	7
Table 1.3: Principle transition in the emission spectrum of Eu(III) (Aspinall, 2001). ...	13
Table 1.4: Principle transitions in the emission spectrum of Tb(III) (Aspinall, 2001)...	13
Table 1.5: Theories of crystal growth (Mulin <i>et al.</i> , 2001).....	16
Table 2.1: List of chemicals and solvents used to synthesizes the lanthanide complexes.....	24
Table 3.1: Yields of the synthesized lanthanide complexes (Ln = Sm, Eu, Tb, Nd).....	32
Table 3.2: Physical appearance, solubility and stability of complexes at ambient condition.....	33
Table 3.3: CHN analysis data of lanthanide (Ln = Sm, Eu, Tb, Nd).....	37
Table 3.4: Crystal data, data collection and structure refinement parameters for the Nd-BAPHEN .....	42
Table 3.5: Selected bond lengths (Å), bond angles (°) for Nd-BAPHEN .....	43
Table 3.6: Hydrogen-bond geometry (Å, °) Cg1, Cg2 and Cg5 are centroids for the C28-C33, C21-C26 and C14-C19 phenyl rings, respectively. Cg3 and Cg4 are the centroids of the N2/C8-C12 and N1/C1-C15 pyridine rings, respectively.....	44
Table 3.7: Crystal data, data collection and structure refinement parameters for the Eu-BAPHEN .....	48
Table 3.8: Selected bond lengths (Å), bond angles (°) for Eu-BAPHEN.....	49
Table 3.9: Hydrogen-bond geometry (Å, °) Cg1 is the centroid of the C35 and C40 benzene ring.....	51

Table 3.10: Crystal data, data collection and structure refinement parameters for the Tb-BAPHEN.....	54
Table 3.11: Selected bond lengths (Å), bond angles (°) for Tb-BAPHEN.....	55
Table 3.12: Hydrogen-bond geometry (Å, °) Cg1 is the centroid of the C35 and C40 phenyl ring.....	57
Table 3.13: Frequency of the absorption bands of the symmetrical and asymmetrical vibrations of COO <sup>-</sup> and the metal-oxygen bond in Ln-BA (Ln = Eu, Nd, Tb, Sm) complexes.....	58
Table 3.14: Frequency of the absorption bands of the symmetrical and asymmetrical vibrations of COO <sup>-</sup> and the metal-oxygen bond in Ln-BA (Ln = Eu, Nd, Tb, Sm) complexes.....	59
Table 3.15: Frequency of the absorption bands of the symmetrical and asymmetrical vibrations of COO <sup>-</sup> and the metal-oxygen bond in Ln-24DCBA (Ln = Eu, Nd, Tb, Sm) complexes.....	61
Table 3.16: Frequency of the absorption bands of the symmetrical and asymmetrical vibrations of COO <sup>-</sup> and the metal-oxygen bond in Ln-HBA (Ln = Eu, Nd, Tb, Sm) complexes.....	62
Table 3.17: Frequency of the absorption bands of the symmetrical and asymmetrical vibrations of COO <sup>-</sup> and the metal-oxygen bond in Ln-BAPHEN (Ln = Eu, Nd, Tb) complexes.....	64
Table 3.18: Decomposition of BA, 24DCBA, 34DCBA, HBA and PHEN.....	65
Table 3.19: Summary of Ln-BA TGA weight loss data.....	67
Table 3.20: Summary of Ln-24DCBA TGA weight loss data.....	69
Table 3.21: Summary of Ln-34DCBA TGA weight loss data.....	70
Table 3.22: Summary of Ln-HBA TGA weight loss data.....	72

Table 3.23: Summary of Eu-BAPHEN, Tb-BAPHEN and Nd-BAPHEN TGA weight loss data. ....	74
Table 3.24: Summary of photoluminescence data of europium complexes. ....	80
Table 3.25: Summary of photoluminescence data of terbium complexes. ....	84

## LIST OF FIGURES

Figure 1.1: Ionic radii of the Ln(III) ions.....	5
Figure 1.2: Energy level diagram for Eu <sup>3+</sup> and Tb <sup>3+</sup> luminescence.....	10
Figure 1.3: Quenching of Eu <sup>3+</sup> emission by $\nu(\text{O-H})$ .....	11
Figure 1.4: Sensitized lanthanide luminescence for europium ion.....	12
Figure 1.5: Equilibrium between carboxyl group and carboxylate ion. ....	15
Figure 1.6: Some possible coordination modes of benzenecarboxylic acid (Ln = lanthanide) (Qu <i>et al.</i> , 2005).....	21
Figure 1.7: Some possible coordination modes of benzenecarboxylic acid with 1,10- phenanthroline (Ln = lanthanide) (Liu <i>et al.</i> , 2005). ....	22
Figure 2.1: Structure of the four carboxylic acids and phenanthroline used in this work. ....	26
Figure 3.1: Molecular structure of Nd-BAPHEN with atomic numbering scheme at 20 % probability displacement ellipsoids for non-H atoms. The suffix A corresponds to the symmetry code [-x, -y+1, -z+1].....	40
Figure 3.2: The crystal structure of Nd-BAPHEN, viewed along the a axis, showing one-dimensional infinite chains along the c axis. Intermolecular hydrogen bonds are shown as dashed lines. ....	41
Figure 3.3: The molecular structure of the title complex, Eu-BAPHEN, showing 20 % probability displacement ellipsoids for the non-H atoms and the atom- numbering scheme. The suffix A corresponds to the symmetry code [- x+2, -y, -z+1].....	46
Figure 3.4: The crystal structure of the title complex, Eu-BAPHEN, viewed along the a axis, showing two chains along a axis. The benzoic acid solvent	

molecules have been omitted for clarity. Intermolecular hydrogen bonds are shown as dashed lines.....	47
Figure 3.5: The molecular structure of the title complex, Tb-BAPHEN, showing 20 % probability displacement ellipsoids for the non-H atoms and the atom- numbering scheme. The suffix A corresponds to the symmetry code [- x+2, -y, -z+2]......	52
Figure 3.6: The crystal structure of the title complex, Tb-BAPHEN, viewed along the a axis, showing four chains along a axis. The benzoic acid solvent molecules have been omitted for clarity. Intermolecular hydrogen bonds are shown as dashed lines.....	53
Figure 3.7: Photoluminescence spectra of a) BA, b) 24DCBA, c) 34DCBA, d) HBA and e) PHEN at room temperature. ....	76
Figure 3.8: Photoluminescence spectra of a) Sm-BA, b) Sm-24DCBA, c) Sm- 34DCBA and d) Sm-HBA at room temperature.....	78
Figure 3.9: Photoluminescence spectra of a) Eu-BA; b) Eu-24DCBA; c) Eu- 34DCBA; d) Eu-HBA; e) Eu-BAPHEN at room temperature. ....	83
Figure 3.10: Photoluminescence spectra of a) Tb-BA; b) Tb-24DCBA; c) Tb- 34DCBA; d) Tb-HBA; e) Tb-BAPHEN at room temperature.....	82
Figure 3.11: Photoluminescence spectra of a) Nd-BA; b) Nd-24DCBA; c) Nd- 34DCBA; d) Nd-HBA; e) Nd-BAPHEN at room temperature.....	85
Figure A-1: FTIR spectra of the ligand BA and complexes of Ln-BA (Ln = Eu, Nd, Tb, Sm).....	104
Figure A-2: FTIR spectra of the ligand 24DCBA and complexes of Ln-24DCBA (Ln = Eu, Nd, Tb, Sm).....	105

Figure A-3: FTIR spectra of the ligand 34DCBA and complexes of Ln-34DCBA (Ln = Eu, Nd, Tb, Sm).....	106
Figure A-4: FTIR spectra of the ligand HBA and complexes of Ln-HBA (Ln = Eu, Nd, Tb, Sm). .....	107
Figure A-5: FTIR spectra of the ligand BA and PHEN.....	108
Figure A-6: FTIR spectra of the ligand HBA and complexes of Ln-HBA (Ln = Eu, Nd, Tb, Sm). .....	109
Figure B-1: TGA spectra of ligand (a), BA; (b), 24DCBA; (c), 34DCBA; (d), HBA; and (e), PHEN.....	114
Figure B-2: TGA spectra of complex (a), Eu-BA; (b), Tb-BA; (c), Nd-BA; (d), Sm-BA. ....	118
Figure B-3: TGA spectra of complex (a), Eu-24DCBA; (b), Tb-24DCBA; (c), Nd-24DCBA; (d), Sm-24DCBA.....	122
Figure B-4: TGA spectra of complex (a), Eu-34DCBA; (b), Tb-34DCBA; (c), Nd-34DCBA; (d), Sm-34DCBA.....	126
Figure B-5: TGA spectra of complex (a), Eu-HBA; (b), Tb-HBA; (c), Nd-HBA; (d), Sm-HBA.....	130
Figure B-6: TGA spectra of complex (a), Eu-BAPHEN; (b), Tb-BAPHEN; (c), Nd-BAPHEN; (d), Sm-BAPHEN.....	133

## LIST OF ABBREVIATIONS/SYMBOL

### Symbols:

Å	angstrom
Å <sup>3</sup>	unit cell volume
Δ	crystal field splitting
μ	descriptor for bridging
κ	hapticity in σ-bonding ligands

### Abbreviations:

23DCBA	2,3-dichlorobenzoic acid
34DCBA	3,4-dichlorobenzoic acid
BA	benzoic acid
BDC	benzenedicarboxylate
CHN	Carbon Hydrogen Nitrogen (elemental analysis)
FTIR	Fourier Transform-Infrared Red
HBA	4-hydroxybenzoic acid
HSBA	hard soft acid base
IUPAC	International Union of Pure and Applied Chemistry
PHEN	1,10-phenanthroline
PL	photoluminescence
SAC	stretch-activated channels
TGA	thermogravimetric analysis
UV	ultraviolet

## LIST OF APPENDICES

Appendix A: FTIR Spectra Of The Ligand And Their Respective Lanthanide-Benzoato Complexes.....	101
Appendix B: TGA Spectra Of The Ligand And Respective Lanthanide-Benzoato Complexes.....	110

# SINTESIS DAN PENCIRIAN KOMPLEKS LANTHANUM-BENZOATO

## ABSTRAK

Enam belas kompleks dan tiga kristal tunggal lanthanum-benzoato disintesis secara refluks biasa dan solvoterma. Struktur tiga kristal tunggal tersebut diciri dengan menggunakan kristalografi sinar-X kristal tunggal.  $[\text{Nd}_2(\text{C}_7\text{H}_5\text{O}_2)_6(\text{C}_{12}\text{H}_8\text{N}_2)_2]$ ,  $[\text{Eu}_2(\text{C}_7\text{H}_5\text{O}_2)_6(\text{C}_{12}\text{H}_8\text{N}_2)_2] \cdot 2(\text{C}_7\text{H}_6\text{O}_2)$  dan  $[\text{Tb}_2(\text{C}_7\text{H}_5\text{O}_2)_6(\text{C}_{12}\text{H}_8\text{N}_2)_2] \cdot 2(\text{C}_7\text{H}_6\text{O}_2)$  mempunyai sistem triklinik dengan kumpulan ruang P-1. Ketiga-tiga kompleks kristal tunggal mempunyai nombor koordinasi 9. Ikatan hidrogen dalam ketiga-tiga kristal menunjukkan interaksi antara molekul dalam kristal tersebut.

Semua kompleks diciri dengan menggunakan analisis unsur, spektroskopi inframerah, analisis termogravimetri dan spektroskopi kependarkilauan. Keputusan FTIR menunjukkan kumpulan karbosilik dalam kompleks telah dikoordinasi dengan ion logam nadir bumi dalam bentuk monodentat dan bidentat dan kumpulan karbosilik ester telah memainkan peranan dalam koordinasi ini. Atom-atom nitrogen dari 1,10-fenantrolin turut mengkoordinasi dalam ion-ion logam nadir bumi kristal unggul dalam bentuk bidentat. Kompleks-kompleks Eu(III) dan Tb(III) menunjukkan pembebasan kependarkilauan yang sangat bagus berbanding dengan yang ditunjukkan oleh kompleks-kompleks Sm(III) dan Nd(III).

Kata kunci: Lantanida-benzoato; Fenantrolin; Struktur kristal; Kependarkilauan

# SYNTHESIS AND CHARACTERIZATION OF LANTHANIDE-BENZOATO COMPLEXES

## ABSTRACT

Sixteen complexes and three single crystals of lanthanide-benzoato were synthesized with normal refluxing and solvothermal method. The structures of the three crystals were characterized using single crystal X-ray crystallography.  $[\text{Nd}_2(\text{C}_7\text{H}_5\text{O}_2)_6(\text{C}_{12}\text{H}_8\text{N}_2)_2]$ ,  $[\text{Eu}_2(\text{C}_7\text{H}_5\text{O}_2)_6(\text{C}_{12}\text{H}_8\text{N}_2)_2] \cdot 2(\text{C}_7\text{H}_6\text{O}_2)$  and  $[\text{Tb}_2(\text{C}_7\text{H}_5\text{O}_2)_6(\text{C}_{12}\text{H}_8\text{N}_2)_2] \cdot 2(\text{C}_7\text{H}_6\text{O}_2)$  all adopted triclinic crystal system with P-1 space group. The three lanthanide-benzoato crystals adopted nine-coordination environment. Hydrogen bonding can be found showing the interaction between molecules in the crystals itself.

All the complexes were characterized by means of elemental analysis, fourier transform infrared-red (FTIR) spectroscopy, thermogravimetric analysis and photoluminescence spectroscopy. The FTIR results show that the carboxylic group in the complexes coordinated to the rare earth ions in the form of monodentate and bidentate, and the ester carboxylic groups have taken part in the coordination. Nitrogen atoms from 1,10-phenanthroline coordinated to the rare earth ions in the single crystal complexes in the form of bidentate as well. Among these complexes, Eu(III) and Tb(III) complexes showed good photoluminescence emission compared with that of Sm(III) and Nd(III) complexes.

Keywords: Lanthanide-benzoato; Phenanthroline; Crystal Structure; Photoluminescence

# CHAPTER 1

## INTRODUCTION

### 1.1 History

“Lanthanons – these elements perplex us in our researches, baffle us in our speculations, and haunt us in our very dreams. They stretch like an unknown sea before us; mocking, mystifying and murmuring strange revelations and possibilities.” – Sir William Crookes, 1887 (Baskerville *et al.*, 1904).

The lanthanides (from the Greek word *lanthanein* meaning “lying hidden”) were once called rare-earth metals (Bunzli *et al.*, 2005). Aspinall (2001) summarised the discovery of lanthanides, when a black mineral called “ytterbite” was found in 1788. Six years later, yttrium was separated from ytterbite by Gadolin. Berzelius isolated cerium from the mineral cerite and found it to have quite similar properties to Gadolin’s yttrium after eight years. In between 1839 and 1843, Mosander discovered erbium and terbium from gadolinite by fractional precipitation with ammonia and lanthanum from cerite by ignition and extraction with diluted nitric acid (Topp *et al.*, 1965). He also isolated a mineral composed of praseodymium and neodymium. In 1937, promethium was discovered as an isotope resulting from the bombardment of neodymium with deuterons in a cyclotron (Cotton *et al.*, 1991). Promethium was synthesized and characterized in 1947, completing the whole lanthanide series. Some of the history of the lanthanides is summarized in Table 1.1.

Table 1.1: History of the lanthanides (Aspinall, 2001)

Element	Discoverer	Date
Cerium, Ce	C.G. Mosander	1839
Lanthanum, La	C. G. Mosander	1839
Praseodymium, Pr	C.A. von Welsbach	1885
Neodymium, Nd	C.A. von Welsbach	1885
Samarium, Sm	L. de Boisbaudran	1879
Europium, Eu	E.A. Demarcay	1901
Yttrium, Y	C.G. Mosander	1843
Terbium, Tb	C.G. Mosander	1843
Erbium, Er	C.G. Mosander	1843
Ytterbium, Yb	J.C.G. de Marignac	1879
Scandium, Sc	L.F. Nilson	1879
Holmium, Ho	P.T. Cleve	1879
Thulium, Tm	P.T. Cleve	1879
Gadolinium, Gd	J.C.G. de Marignac	1880
Dysprosium, Dy	L. de Boisbaudran	1886
Lutetium, Lu	G. Urbain C.A von Welsbach	1907
Promethium, Pm	J.A. Marinsky L.E. Glendenin C.D. Coryell	1947

## 1.2 General Information about Lanthanides

The lanthanide series consists of 15 elements with atomic numbers 57 through 71, which differentiate them from the d-block metals. The coordination geometries of lanthanide complexes are determined by ligand steric factors rather than crystal field effect. They also tend to have small crystal-field splitting and very sharp electronic spectra (Cotton *et al.*, 2006). Lanthanide elements exhibit unique physical and chemical properties, and are widely used in laser and fluorescent materials because these elements deflect ultraviolet and infrared radiation. Other applications such as catalytic converters, petroleum refining catalysts, magnetic substances, ceramics and so forth have been produced using lanthanide elements (Morgan and Mitchell *et al.*, 2007; Bleaney *et al.*, 1973). Luminescent lanthanide complexes have played an important role from lighting and light conversion technology to biomedical and sensing areas.

### 1.2.1 Oxidation States

The most stable and dominant oxidation state of lanthanides is +3, resulting from the effect of increasing positive charge on the valence orbital. The orbitals are stabilized in the order of  $4f > 5d > 6s$  when electrons are removed from a Ln atom. Further removal of electrons from the 4f orbital is energetically unfavorable. The +2 and +4 oxidation states are formed by elements that can attain empty, half-filled or filled 4f shells.

Dipositive lanthanides, samarium ( $f^6$ ), europium ( $f^7$ ), thulium ( $f^{13}$ ) and ytterbium ( $f^{14}$ ) have been prepared and characterized including the dihalides except for  $\text{LnF}_2$  (Mikheev *et al.*, 1988).  $\text{Sm}^{2+}$ ,  $\text{Eu}^{2+}$  and  $\text{Yb}^{2+}$  have some aqueous chemistry

but are oxidized by air.  $\text{Sm}^{2+}$  is relatively unstable and exhibits strong reducing power while  $\text{Tm}^{2+}$  is an extremely unstable species.

The +4 oxidation state is significant only for  $\text{Ce}^{4+}$  ( $f^0$ ),  $\text{Pr}^{4+}$  ( $f^1$ ), and  $\text{Tb}^{4+}$  ( $f^7$ ). Among them  $\text{Ce}^{4+}$  is the most stable and has a significant aqueous chemistry. Ce, Pr and Tb also form oxides and fluorides.

The redox properties of the lanthanides depend on not just the electronic factors such as the inherent stability of the f shells but also the medium (e.g. solvent and pH) and types of ligand attached to the element (Imamoto *et al.*, 1994).

### 1.2.2 Ionic Radius

The ionic radii of the lanthanides are larger than those of the d-block transition elements. They decrease smoothly across the series (Figure 1.1) due to the lanthanide contraction, which refers to the fact that the 5s and 5p orbitals penetrate the 4f sub-shell so the 4f orbital is not shielded from the increasing nuclear charge, and causes the atomic radius of the atom to decrease. This decrease in size continues throughout the series (Cotton *et al.*, 1966).

The smooth decrease in the ionic radii results in a regular variation in chemical properties. The relatively large ionic radii of the lanthanides allow the accommodation of up to 12 ligands in the sphere, and coordination numbers of 7, 8 and 9 are common (Thompson *et al.*, 1979; Cotton *et al.*, 2005; Strobel and Schleid *et al.*, 2006). In general, ‘light’ lanthanides (atomic number: 57-64), whose ionic radii are large, tend to have higher coordination numbers than ‘heavy’ lanthanides (atomic number: 65-71).

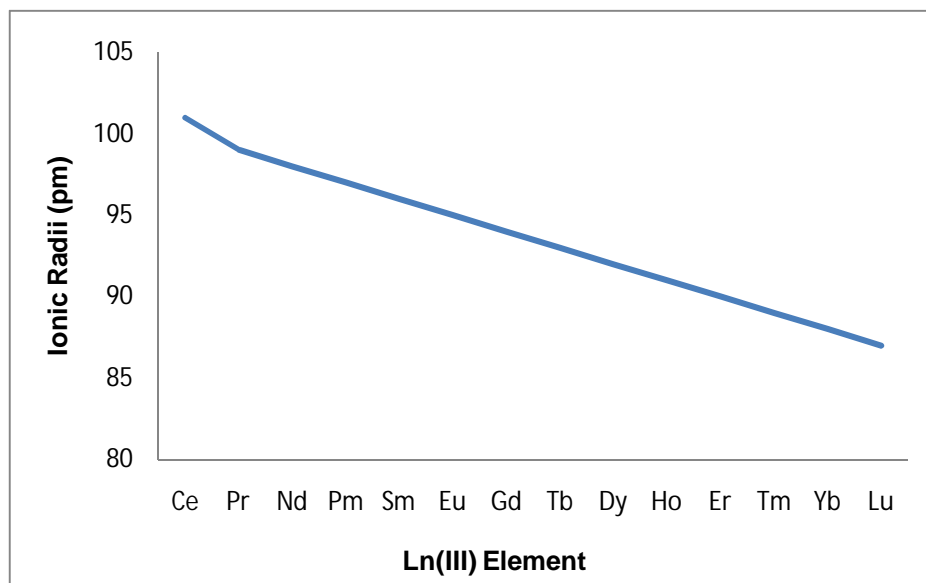


Figure 1.1: Ionic radii of the Ln(III) ions.

### 1.2.3 Magnetic Properties

Bunzil and Choppin (1989) have reported that all of the trivalent lanthanide ions with the exception of  $\text{La}^{3+}$  ( $f^0$ ) and  $\text{Lu}^{3+}$  ( $f^{14}$ ) are paramagnetic. Due to their strong localization, the 4f electrons are located almost completely inside the occupied 5s and 5p shells and hence do not contribute to chemical bonding. The orbital contribution of the electron towards magnetic moment is usually quenched by interaction with electric fields of the environment in transition elements but in case of lanthanides the 4f orbitals lie too deep in the atom for such quenching to occur. Therefore, the spin moments of these transition cations determine the paramagnetism, which has a maximum value that coincides with the maximum number of unpaired electrons in the 3d orbitals.

### 1.2.4 Optical Properties

Three type of electronic transitions that occur in the lanthanides are the  $f \rightarrow f$ ,  $nf \rightarrow (n+1)$  and ligand  $\rightarrow$  metal  $f$  charge transfer. The field of the surrounding anions and dipolar molecules will affect the shielding of the  $f$  orbitals of a lanthanide cation. This will results in minimal perturbation of the electronic transition between the energy levels of these  $f$  orbitals. In contrast to the broad  $d \rightarrow d$  absorption bands of the transition elements, the  $f \rightarrow f$  bands of the lanthanides in solids and solution are almost as narrow as they are for the gaseous ions and are less perturbed by complexation when producing the ligand field effects. The  $f \rightarrow f$  transitions are electric-dipole forbidden by the Laporte selection rule, which causes weak intensities. The forbidden  $f \rightarrow f$  bands intensities are increased in non-centrosymmetric systems by the mixture of a degree of  $d$  orbital character with the  $f$  states and the centrosymmetric systems can have the intensities enhanced by coupling the  $f$  electronic states with a vibrational state, thereby removing the center of symmetry (Aspinall, 2001).

From the principal  $f \rightarrow f$  absorption bands and the resultant colours of the  $\text{Ln}^{3+}$  ions, the luminescence spectra show groups of narrow lines ascribed to transitions inside the  $4f$  shell, that in solution can somewhat broaden. The number of possible transitions increases with the number of unpaired electrons, so the number and pattern of the bands have an inverse symmetry after  $\text{Gd}^{3+}$ . Thus, the lowest seven levels of  $\text{Eu}^{3+}$  are, in order of increasing energy,  $J = 0, 1, 2, 3, 4, 5, 6$  while those  $\text{Tb}^{3+}$  are  $J = 6, 5, 4, 3, 2, 1, 0$ . In addition to the transition listed (Table 1.2),  $\text{Ce}^{3+}$ ,  $\text{Pr}^{3+}$ ,  $\text{Tb}^{3+}$ ,  $\text{Sm}^{3+}$  and  $\text{Yb}^{3+}$  have rather intense absorption peaks in the near-UV to visible range, which are associated with  $f \rightarrow d$  transitions.

Table 1.2: Summary of the properties of Ln(III) ions.

Ln <sup>3+</sup>	4f <sup>n</sup>	Ground level	Colour	Absorption bands (nm)
Ce	1	<sup>2</sup> F <sub>5/2</sub>	Colourless	None
Pr	2	<sup>3</sup> H <sub>4</sub>	Green	444.5, 469.0, 482.2, 588.5
Nd	3	<sup>4</sup> I <sub>9/2</sub>	Lilac	345.0, 521.8, 574.5, 739.5, 742.0, 797.5, 803.0, 868.0
Pm	4	<sup>5</sup> I <sub>4</sub>	Pink	548.5, 568.0, 702.5, 735.5
Sm	5	<sup>6</sup> H <sub>5/2</sub>	Yellow	362.5, 374.5, 402.0
Eu	6	<sup>7</sup> F <sub>0</sub>	Pale pink	375.5, 394.1
Gd	7	<sup>8</sup> S <sub>7/2</sub>	Colourless	272.9, 273.3, 275.4, 275.6
Tb	8	<sup>7</sup> F <sub>6</sub>	Pale pink	284.4, 350.3, 367.7, 487.2
Dy	9	<sup>6</sup> H <sub>15/2</sub>	Yellow	350.4, 365.0, 910.0
Ho	10	<sup>5</sup> I <sub>8</sub>	Yellow	287.0, 361.1, 416.1, 450.8, 537.0, 641.0
Er	11	<sup>4</sup> I <sub>15/2</sub>	Rose-pink	364.2, 379.2, 487.0, 522.8, 652.5
Tm	12	<sup>3</sup> H <sub>6</sub>	Pale green	360.0, 682.5, 780.0
Yb	13	<sup>2</sup> F <sub>7/2</sub>	Colourless	975.0
Lu	14	<sup>1</sup> S <sub>0</sub>	Colourless	None

Ce<sup>3+</sup>, Tb<sup>3+</sup>, Sm<sup>3+</sup>, Eu<sup>3+</sup> and Yb<sup>3+</sup> have more intense and broader bands, as these are f → d transitions. Certain f → f bands of Ln<sup>3+</sup> ions experience relatively large changes in shape and/or intensity when changes occur in the coordination sphere of the ion. These “hypersensitive” bands generally follow a ΔJ = 2 selection rule and have been shown to be of use in studying lanthanide complexation.

### 1.2.5 Toxicity

Detailed toxicological studies of lanthanides are necessary due to the fact that lanthanides are able to penetrate into the human body. La<sup>3+</sup> and Gd<sup>3+</sup> block different

calcium channels in human and animal cells (Wadkins *et al.*, 1998). For example,  $Gd^{3+}$  blocks stretch-sensitive ionic channels (SAC) in the sarcolemma of skeletal muscle fibers (Coirault *et al.*, 1999).  $Dy^{3+}$  and  $La^{3+}$  block  $Ca^{2+}$ -ATPase and  $Mg^{2+}$ -ATPase (Van der Laarse *et al.*, 1995). It is suggested that  $Dy^{3+}$  inhibits this enzyme much more than other lanthanide ions.  $Eu^{3+}$  and  $Tb^{3+}$  inhibit calcineurin (Burroughs *et al.*, 1994).  $Eu^{3+}$  is able to replace  $Ca^{2+}$  bound to calcineurin. The binding of  $Tb^{3+}$  by calcineurin is slightly weaker. It seems that lanthanides significantly affect biochemical pathways, thus altering physiological processes in the tissues of humans and animals.

### 1.2.6 Occurrence

Lanthanides are also known as rare earth metals. However, these elements are not rare, except for promethium which is prepared by neutron irradiation of neodymium. For example, cerium, the most abundant in the lanthanide series, is more abundant than cobalt, tin and zinc; while thulium, which is the least abundant, occurs in similar quantities to mercury and is more abundant than silver. A major mineral source of the rare earths is bastnasite. The rest are monazites and xenotime. These ore deposits are located mainly in China, India, Malaysia, and Sri Lanka. China, especially occupies more than 90 % of the production. Other productive countries are USA, Australia, Canada, South Africa and Brazil (Taylor *et al.*, 1964; Hedrick *et al.*, 2004). Separation of each element has been established on an industrial scale, and all the lanthanides except for promethium, are available as metal ingots or as powders, oxides and salt.

### 1.3 Lanthanide Luminescence

The simplest photoluminescence process is resonant radiation, in which a photon of a particular wavelength is absorbed and an equivalent photon is immediately emitted. This process does not involve any internal energy transitions of the chemical substrate between absorption and emission. The process happens in the count of nanoseconds. Fluorescence and phosphorescence are the emissions of photons after a sample has been excited by electromagnetic radiation; the distinction between the two is that fluorescence is a spin allowed process taking  $10^{-6}$  to  $10^{-12}$  s whereas phosphorescence involved a change in spin multiplicity and is a slower process, taking from  $10^{-6}$  s to as much as several seconds. The term ‘luminescence’ will be used here to describe both fluorescence and phosphorescence.

When the lanthanides exhibit intense luminescence, applications ranging from biomedical (Yam *et al.*, 1999) to sensing areas (Beeby *et al.*, 2000) and optical imaging (Faulkner *et al.*, 2005) become possible, which are based on the long-lived excited states of lanthanide ions. They can exhibit quite intense visible line-like emissions, long known from an exceptionally extended literature.  $\text{Nd}^{3+}$ ,  $\text{Yb}^{3+}$  and  $\text{Er}^{3+}$  can emit longer-wavelength emission and are more efficient in penetrating human tissue than visible light, thus convenient medical diagnostic procedures can be conceived based on long-wave emitters.

The energy level diagrams for  $\text{Eu}^{3+}$  and  $\text{Tb}^{3+}$  luminescence are shown in Figure 1.2 as an example. The excitation of  $\text{Ln}^{3+}$  to an emissive state by this route is not an efficient process due to Laporte forbidden, which is the  $f \rightarrow f$  transition. However, once the ion has been excited to the emissive state by ligand, luminescence process can occur. The rate of non-radiative de-excitation is strongly related to the

size of the energy gap between lowest emissive state and the highest state of the ground manifold.

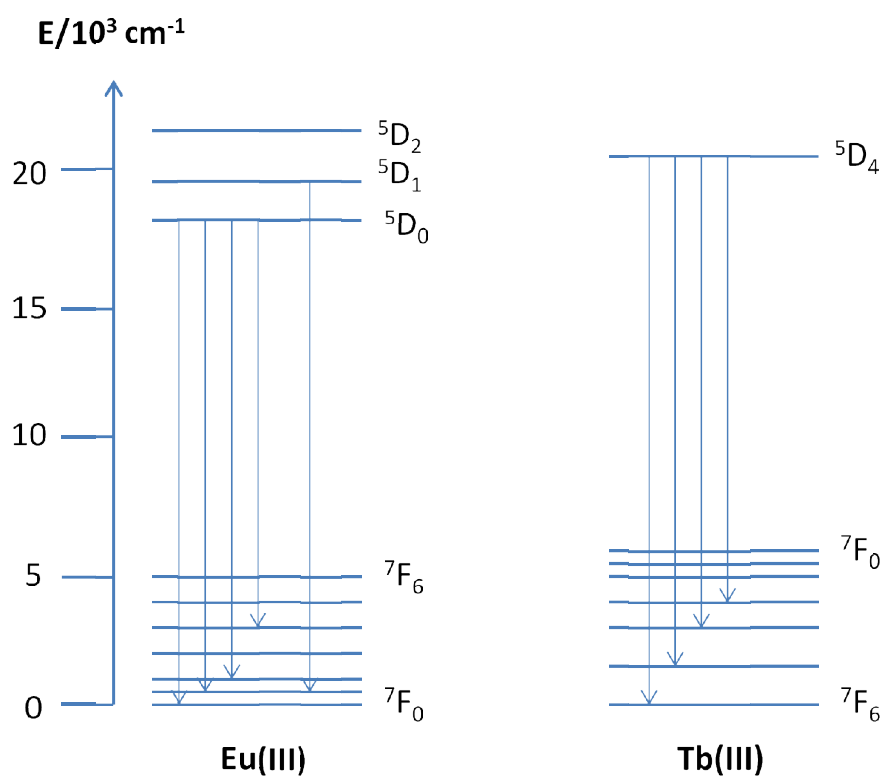


Figure 1.2: Energy level diagram for  $\text{Eu}^{3+}$  and  $\text{Tb}^{3+}$  luminescence (Aspinall, 2001)

The energy gap in every lanthanide can be bridged by weak vibronic coupling of the excited state with high frequency oscillators such as an overtone of the  $\nu(\text{O-H})$  vibration of coordinated  $\text{H}_2\text{O}$  molecules. For example, the energy gap for  $\text{Eu}^{3+}$  is bridged by three quanta of O-H vibrational energy as shown in Figure 1.3. As for  $\text{Tb}^{3+}$ , four quanta are required to bridge the corresponding gap. As a result of this facile de-excitation pathway, luminescence is not observed for aqueous solutions of  $\text{Eu}^{3+}$  or  $\text{Tb}^{3+}$ . Quenching of the excited states in  $\text{D}_2\text{O}$  solution is less effective than in  $\text{H}_2\text{O}$  as five quanta of the lower energy  $\nu(\text{O-D})$  are needed to bridge the energy gap

for  $\text{Eu}^{3+}$  and six for  $\text{Tb}^{3+}$ . Efficient luminescence requires that the lanthanide ions be well separated from any high frequency oscillators (Aspinall, 2001).

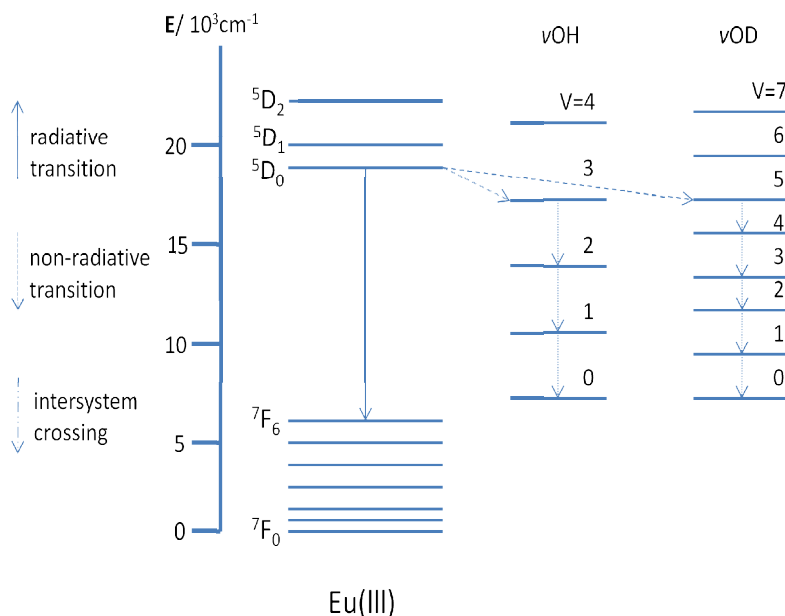


Figure 1.3: Quenching of  $\text{Eu}^{3+}$  emission by  $\nu(\text{O-H})$  (Aspinall, 2001).

### 1.3.1 Sensitized Luminescence

The efficiency of lanthanide luminescence can be enhanced by increasing the efficiency of excitation in lanthanides. Direct excitation to the emissive level cannot be an efficient process because  $f \rightarrow f$  transitions are Laporte forbidden. An alternative method of excitation is via an antenna (chromophore). The antenna can be any aromatic or hetero-aromatic highly  $\pi$ -conjugated system characterized by high efficiency of light absorption and high efficiencies of intersystem crossing and energy transfer processes. The efficiency of a chromophore to behave as a sensitizer is related to the energy of its triplet excited state, which should be at least  $1850 \text{ cm}^{-1}$  higher than the lowest emitting levels of the  $\text{Ln}^{3+}$  cation (Latva *et al.*, 1997).

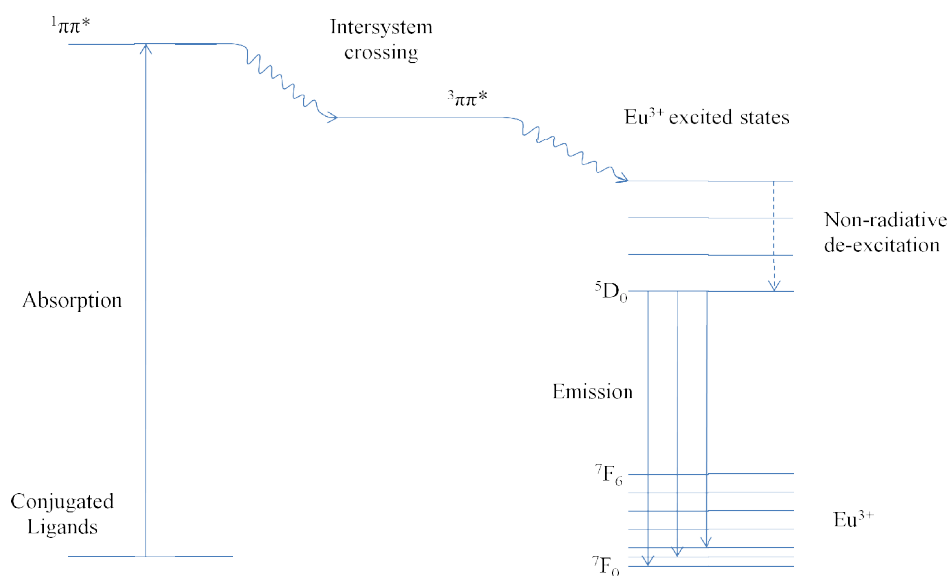


Figure 1.4: Sensitized lanthanide luminescence for europium ion.

### 1.3.2 Luminescence Spectroscopy

There are two types of luminescence spectroscopy. The first type is the excitation spectroscopy. The intensity of a single emission is monitored while scanning excitation frequency. The second type is the emission spectroscopy, where the sample is irradiated with a fixed excitation frequency while the intensity and frequency of the emitted photons is scanned. For  $\text{Eu}^{3+}$  the most important emissive state is  $^5\text{D}_0$  and for  $\text{Tb}^{3+}$  it is  $^5\text{D}_4$ ; the properties of the most important transitions are summarized in Table 1.3 and 1.4.

In addition, due to the different quenching effects of  $\text{D}_2\text{O}$  and  $\text{H}_2\text{O}$ , the measurements of luminescence lifetimes in  $\text{D}_2\text{O}$  and  $\text{H}_2\text{O}$  can allow the estimation of the number of coordinated  $\text{H}_2\text{O}$  molecules in a complex (Turta *et al.*, 2007).

Table 1.3: Principle transition in the emission spectrum of Eu(III) (Aspinall, 2001).

Transition	Range	Intensity	Comments
${}^5D_0 \rightarrow {}^7F_0$	577 - 581	Very weak	Forbidden, non-degenerate: if more than one transition appears then more than one Eu containing species is present
${}^5D_0 \rightarrow {}^7F_1$	585 - 600	Strong	Allowed, intensity independent of environment, strong optical activity
${}^5D_0 \rightarrow {}^7F_2$	610 - 625	Strong to very strong	Hypersensitive, absent if ion lies on inversion centre
${}^5D_0 \rightarrow {}^7F_3$	640 - 657	Very weak	Forbidden, always very weak, J mixing adds an allowed magnetic dipole character
${}^5D_0 \rightarrow {}^7F_4$	680 - 710	Medium to strong	Sensitive to Eu environment
${}^5D_1 \rightarrow {}^7F_1$	530 - 540	Very weak	Sensitive to Eu environment

Table 1.4: Principle transitions in the emission spectrum of Tb(III) (Aspinall, 2001).

Transition	Range	Intensity	Comments
${}^5D_4 \rightarrow {}^7F_6$	480 - 505	Medium to strong	Sensitive to Tb environment
${}^5D_4 \rightarrow {}^7F_5$	535 - 555	Strong to very strong	Best transition for these as probe
${}^5D_4 \rightarrow {}^7F_4$	580 - 600	Medium to strong	Sensitive to Tb environment
${}^5D_4 \rightarrow {}^7F_3$	615 - 625	Medium	Display strong optical activity
${}^5D_4 \rightarrow {}^7F_2$	640 - 655	Weak	Sensitive to Tb environment

## 1.4 Coordinating Ligands of Lanthanide Complexes

### 1.4.1 Carboxylic Acid – General Properties

A carboxylic acid contains a carboxyl group,  $\text{-COOH}$ , which has one oxygen atom doubly bonded to the carbon atom and a hydroxy (OH) group singly bonded to the carbon atom. The carbon atom of the carboxyl group must also be attached to an organic group or a hydrogen. Carboxylic acids are referred to as oxoacids by having the structure of  $\text{RC=OOH}$  (Acclabs, 2006) by IUPAC standard.

Carboxylic acids are generally polar molecules which dissolve in polar organic solvents. A short-chain aliphatic acid appears as pungent, corrosive and water-soluble liquid with abnormally high boiling point due to hydrogen bonding interactions. As the molecular weight increases in parallel to the increasing dominance of hydrocarbon grouping, the sharpness of odor and water solubility diminishes, while the boiling and melting point rises. The carboxyl group ionizes to form negative carboxylate ions,  $\text{RCOO}^-$  (Figure 1.4). The stability and formation of carboxylate ion depend mainly on its resonance and the inductive effect contributed by electron-withdrawing and electron-donating group presents within the molecular carboxylate ion. The presence of such groups near the  $\text{-COOH}$  group of a carboxylic acid has an effect on the acidity and the tendency to form carboxylate ion. In general, electron-withdrawing groups increase the acidity by increasing the stability of the carboxylate ion.

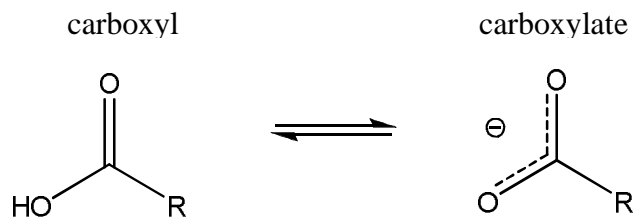


Figure 1.5: Equilibrium between carboxyl group and carboxylate ion.

## 1.5 Crystalline Materials and Single Crystals

### 1.5.1 Definition of Crystal and Single Crystal

A single crystal is a material where the crystal lattice of the entire sample is continuous, unbroken to the edges of the sample with no grain boundaries and is composed of a pattern, a set of atoms arranged in a particular way, and a lattice exhibiting long-range order and symmetry. The definition of crystalline materials refers to materials with a high degree of characteristic three-dimensional translation repetition of basic structural pattern. This may be comprised of a single atom or molecule or a complex assembly of molecules (Glusker *et al.*, 1972; Howard *et al.*, 1998). The orderly arrangement of internal structure gives crystalline materials a distinct sharp melting temperature at a given pressure as compared to amorphous solids which melt over a certain temperature range. Therefore, single crystals are crystalline materials which fulfill the requirement stated in the definition. In addition, it must consist of only single phase, pure and defect-free crystals.

There are as many as 230 space groups and for most molecules, statistics show that 95 % of all compounds crystallize out in these 16 space groups: monoclinic P21/c, P21, P21/m, P2/c, C2/c, C2/m, Cc, C2, the triclinic P-1, P1, and the orthorhombic P212121, Pbca, Pnma, Pna21, Pbcn, Pca21 and P21212.

## 1.5.2 Crystal Growth Theories

Crystal growth is a crystallization process of a solid, and growth into the characteristic arrangement of a crystalline Bravais lattice. The initial stage of nucleation is either homogeneous or heterogeneous. Literature review shows that most of the present nucleation and crystal growth theories were devised during research activities in the past and were subsequently modified to suit anomalies and deviations observed experimentally. Nucleation processes were studied with various techniques available, such as *in situ* hot stage optical microscopy (Krumme *et al.*, 2004), *in situ* hot stage atomic force microscopy (Beekmans *et al.*, 2000) and others (Anisimov *et al.*, 2003).

The proposed mechanisms of crystal growth were discussed broadly under a few general theories; the surface energy theories, the diffusion theories, the adsorption-layer theories and so on (Mulin *et al.*, 2001). Table 1.5 summarizes some of the common crystal growth theories.

Table 1.5: Theories of crystal growth (Mulin *et al.*, 2001)

Theory	Theorist	Year of Conception
Surface Energy Theory	Gibbs	-----
<b>Definition:</b> The shape of growing crystal is that which has a minimum surface free energy in equilibrium with its surroundings at constant temperature and pressure.		
Adsorption-layer Theory, Volmer's Theory or Gibbs-Volmer Theory	Volmer	1939
<b>Definition:</b> The shape of growing crystal is that which has a minimum surface free energy in equilibrium with its surroundings at constant temperature and pressure.		

Kinematic Theory	Frank	1958
<b>Definition:</b> Crystal growth as two processed that involved in the layer growth of crystals. Involves the generation of steps at some source on the crystal face followed by the movement of layers across the face, the movement of macrosteps of unequal distance apart.		
Diffusion-Reaction Theory	Noyes and Whitney	1897
<b>Definition:</b> Considered that the deposition of solid on the face of a growing crystal was essentially a diffusional process and the reverse of dissolution, and that the rates of both processes were governed by the difference between concentration at the solid surface and in the bulk of the solution.		

### 1.5.3 Solution Growth of Single Crystal

The production of large single crystal is broadly divided into three general methods, namely growth from solutions (Sangwal *et al.*, 1994), growth from melts (Smirnova *et al.*, 2004) and growth from vapors (Libbrecht *et al.*, 2005). There are many variations in the processing techniques available within these three groups such as Czochralski (CZ) (O'Mara *et al.*, 1980), Bridgman (Chen *et al.*, 2005), various floating zone methods (Yudin *et al.*, 1997), electron beam drip melting (Giebovsky *et al.*, 1995) and strain annealing (Donald *et al.*, 1975). Other common techniques include slow evaporation, slow cooling, vapor diffusion, solvent diffusion, etc.

### 1.5.4 Hydrothermal Growth/Synthesis

The hydrothermal technique is used to synthesize and crystallize substances from high-temperature aqueous solutions at high vapor pressures. This technique delivered quite promising single crystal growth for most of the highly stable

lanthanide carboxylate complex involving any type of framework structure (Reineke *et al.*, 1999a; 1999b; Wan *et al.*, 2003). Many interesting phenomena such as ligand oxidative coupling, hydrolysis, substitution, redox and decarboxylation can occur under hydrothermal conditions. Water is used in crystal growing as the technique is called hydrothermal, whereas the technique is called solvothermal if organic solvent is used besides water. The principle of the method is based on an appreciable increase of solubility of the targeted complexes in water at elevated temperatures and pressures. Various authors have explained the hydrothermal crystal growth technique and hydrothermal equipment in detail (Lobachev *et al.*, 1973; Demianets *et al.*, 1991; Hoyle *et al.*, 1992).

Complex formation is strongly influenced by the reaction conditions of the hydrothermal approach, especially the reaction temperature and duration. The material must be thermodynamically stable and have sufficient solubility to permit reasonable supersaturation for crystallization to occur (Mullin *et al.*, 2001).

## **1.6 Complexation between Carboxylic Acid and Lanthanide**

### **1.6.1 Coordination Chemistry of Lanthanide**

A review that describes the basic principles for the design of organic ligands for alkali and alkali-earth cations has been reported by Lehn in 1973. The ligand topology (dimensionality, connectivity, size), the binding sites (electronic, properties), the layer properties (rigidity), the environment properties and counterion effect are particularly important parameters in order to achieve control over chemical, structural and thermodynamic properties of a complex. In general, attraction between a ligand and a metal cation results in complex formation and is often associated with

their partial or total desolvation. Research in coordination of lanthanide carboxylate complexes has intensified in the last few decades for the advancement for understanding in its chemistry and in search of potentially new and improved applications (Bunzli *et al.*, 1989).

Rare earth elements have been long under scrutiny in view of important applications, which are based on the exploitation of their magnetic or luminescence features. Lanthanide ions also display diverse coordination modes resulting in the presence of variable and high coordinate number (Aspinall, 2001). Europium and terbium are known for their photoluminescence, which can be further enhanced by highly absorbing chromophores as mentioned in section 1.3.

Lanthanum, the second most abundant lanthanides after cerium, is the first member of the lanthanide family with the electronic configuration of  $[\text{Xe}]4f^05d^16s^2$ . Therefore La(III) has the easiest accessible valence state and the chemistry of La(III) species is the prototype for the behavior of all the trivalent, lanthanides (Morss, 1976; Moeller, 1963; Vickery, 1953). Gadolinium (Gd) has the stable  $4f^7$  configuration. These seven unpaired electrons give rise to a high magnetic moment property which is suitable to be used as injectable contrast agent in magnetic resonance imaging (Sherry *et al.*, 1989). The extra-stable half-full 4f shell, with no low lying energy levels, also has been applied as an inert phosphor host (Tb:Gd<sub>2</sub>O<sub>2</sub>S) for X-ray cassettes (Brixner *et al.*, 1987).

Various ligands and chelates had been attempted in the effort to create new crystal structures for newly and improved application. These include carboxylate (Liu *et al.*, 2008), phosphonate (Ma *et al.*, 2008), diketone (Yan *et al.*, 2008) and mixed-type ligands. Lanthanides carboxylates have been widely studied by various researchers. In the present research, a number of carboxylic acids alone or mixed

with phenanthroline are used as coordination ligands with selected lanthanide salts present.

### **1.6.2 Hard Soft Acid Base (HSAB) Principle Character of Tripositive Lanthanide Cations ( $\text{Ln}^{3+}$ )**

The HSAB theory (also known as Pearson Acid-Base Concept), defines a soft base as a donor in which valence electrons are easily distorted, polarized or removed while a hard base has the opposite properties (Pearson *et al.*, 1968a; 1968b; 1995). A hard acid is an acceptor with small ion/atom size, high positive charge and with no valence electrons that are easily distorted while a soft acid is referred as an acceptor ion/atom with a large size, small or zero positive charge or has several valence electrons which are easily distorted. In general, the HSAB principle states that hard acids generally coordinate with hard bases and vice versa.

Based on the classification of HSAB theory,  $\text{Ln}^{3+}$  cations act as typical hard acids and interact preferentially with hard bases and donor atoms such as fluoride or oxygen atoms from carboxyl group or nitro groups. However, the lanthanide cations can also interact with the softer donors such as nitrogen, sulfur, phosphorous in organic solvents of low solvating power. In aqueous solutions, interaction between  $\text{Ln}^{3+}$  and nitrogen donor sites can occur for ligands such as the aminopolycarboxylates. Thus, softer donors are able to interact with  $\text{Ln}^{3+}$  to eliminate the competition of hydrated water molecules.

## 1.7 Complexation with Aromatic Carboxylic Acid/1,10-phenanthroline with Lanthanide

Benzoic acid and its derivatives are the simplest aromatic carboxylic acids which act as monodentate or bidentate ligands and will generate simple structures with lanthanides. Addition of another ligand, 1,10-phenanthroline, which is a bidentate ligand, will replace some of the benzoic acid in the complex and create a new structure. The intra- and intermolecular hydrogen bonding with methyl, hydroxyl and others, further contributes to the crystal packing. Some of these possible coordination modes are shown in Figures 1.6 and 1.7.

Complexation of lanthanides by mixing aromatic carboxylic acids with N-containing heterocyclic compounds known to be highly absorbing chromophores enhance the photoluminescence properties of lanthanides.

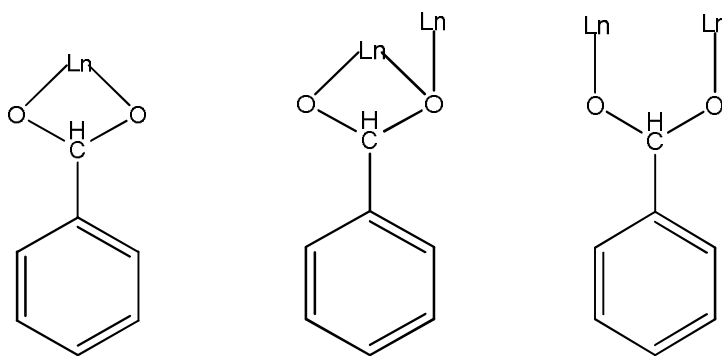


Figure 1.6: Some possible coordination modes of benzenecarboxylic acid (Ln = lanthanide) (Qu *et al.*, 2005).

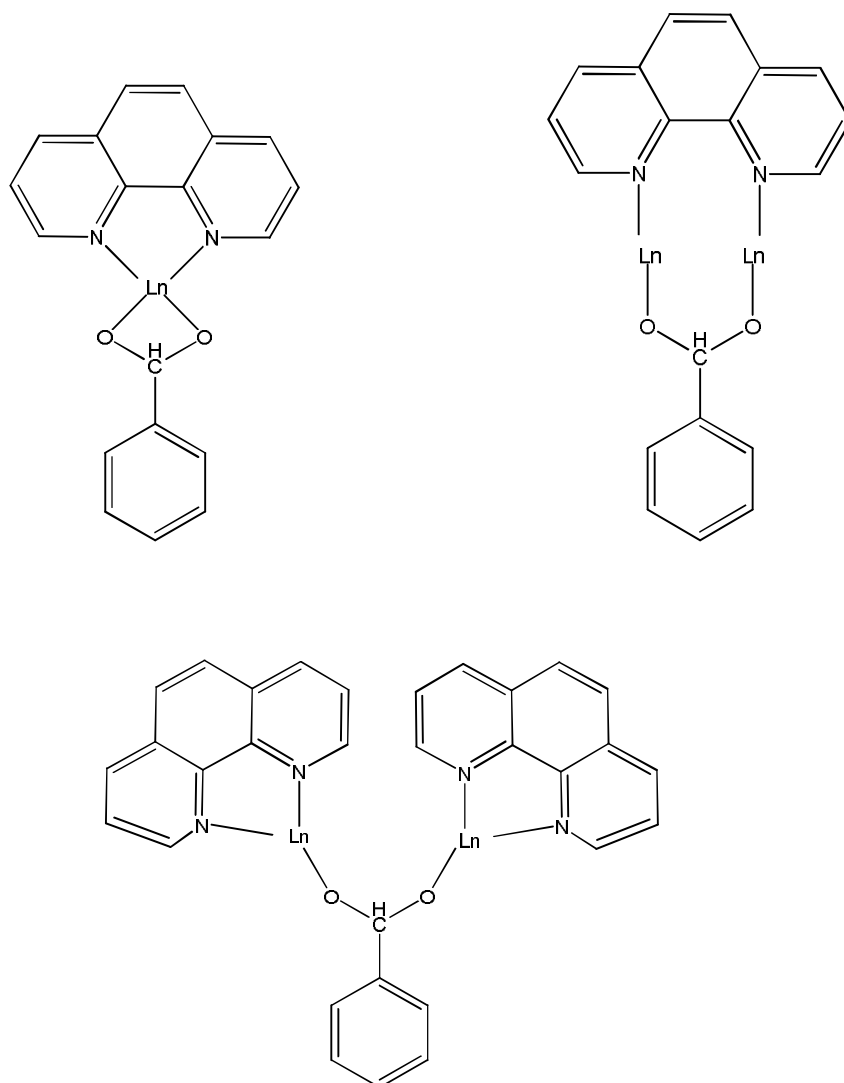


Figure 1.7: Some possible coordination modes of benzenecarboxylic acid with 1,10-phenanthroline (Ln = lanthanide) (Liu *et al.*, 2005).

## 1.8 Research Objective

The first objective of this research is to synthesize lanthanide (Ln = Nd<sup>III</sup>, Eu<sup>III</sup>, Sm<sup>III</sup> and Tb<sup>III</sup>) complexes by using the chosen carboxylic acids which are benzoic acid (BA), 2,4-dichlorobenzoic acid (24DCBA), 3,4-dichlorobenzoic acid (34DCBA) and 4-hydroxybenzoic acid (HBA). A second set of lanthanide (Ln =

Nd<sup>III</sup>, Eu<sup>III</sup> and Tb<sup>III</sup>) complexes will be synthesized using mixed ligands, benzoic acid and 1,10-phenanthroline.

The second objective is to characterize and determine the structure of the complexes obtained by using single crystal X-ray diffraction technique, solid state FTIR and CHN elemental microanalysis. Various structural properties such as bond lengths and bond angles, coordination modes of ligands, coordination number of lanthanide ions, bonding interactions and crystal packing mode will be evaluated and described. These results will be compared and correlated with presently available literature data to identify similarities, differences and new features of the crystal structures.

The third objective of this research is to investigate the thermal properties, stabilities and photoluminescence (PL) properties of the lanthanide complexes.

**CHAPTER 2**  
**EXPERIMENTAL**

**2.1 Materials**

Table 2.1 lists all chemicals used throughout the experiments and the chemical structures of the free ligands are illustrated in Figure 2.1. All chemicals were not further purified unless stated otherwise.

Table 2.1: List of chemicals and solvents used to synthesizes the lanthanide complexes.

<b>Name</b>	<b>Formula</b>	<b>Molecular weight (g/mol)</b>	<b>Purity/Grade</b>	<b>Supplier</b>
Neodymium oxide	Nd <sub>2</sub> O <sub>3</sub>	336.47	99.90 %	Acros Organics
Europium oxide	Eu <sub>2</sub> O <sub>3</sub>	351.92	99.90 %	Acros Organics
Samarium oxide	Sm <sub>2</sub> O <sub>3</sub>	348.72	99.90 %	Sigma
Terbium oxide	Tb <sub>2</sub> O <sub>3</sub>	365.85	99.8 %	Sigma
Benzoic Acid	C <sub>7</sub> H <sub>6</sub> O <sub>2</sub>	122.12	99.0 %	Acros Organics
2,4-dichlorobenzoic acid	C <sub>7</sub> H <sub>4</sub> Cl <sub>2</sub> O <sub>2</sub>	191.01	99.0 %	Acros Organics
3,4-dichlorobenzoic acid	C <sub>7</sub> H <sub>4</sub> Cl <sub>2</sub> O <sub>2</sub>	191.01	99.0 %	Acros Organics
4-hydroxybenzoic acid	C <sub>7</sub> H <sub>6</sub> O <sub>3</sub>	138.12	99.0 %	Acros Organics
1,10-phenanthroline	C <sub>12</sub> H <sub>8</sub> N <sub>2</sub> ·H <sub>2</sub> O	198.23	98 %	Sigma